

Nonresonant Multiphoton Ionization of Noble Gases: Theory and Experiment

M. D. Perry, A. Szoke, O. L. Landen, and E. M. Campbell

*Lawrence Livermore National Laboratory, University of California,
Livermore, California 94550*

(Received 21 July 1987)

The absolute yields of multiply charged ions of the noble gases argon, krypton, and xenon as functions of laser intensity at $\lambda = 586$ nm is reported. The measurements were performed with a well characterized picosecond dye laser in the range 10^{13} to 4×10^{14} W/cm². Charge states up to Ar⁺⁴, Kr⁺⁵, and Xe⁺⁶ were observed at the highest intensities. An extension of the Keldysh-Reiss-Faisal theory which accounts for the Coulomb field of the residual ion is presented and found to be in good agreement with the experimental results with no adjustable parameters.

PACS numbers: 32.80.Rm, 32.80.Wr

Amplified, short-pulse dye laser systems provide a hitherto underutilized laser source for the study of the interaction of intense light ($> 10^{13}$ W/cm²) with atoms or molecules under collisionless conditions. Provided that the laser can be well diagnosed and the focal intensity distribution well characterized, dye laser systems are a nearly ideal intense light source since the laser frequency may be tuned over a considerable range. This provides the capability to investigate the influence of intermediate resonances in multiphoton ionization. In this Letter, we report the first measurement of multiphoton ionization in the 10^{14} -W/cm² intensity range using such a laser, and describe a theory which is in quantitative agreement with the experimental data.

Here, we concentrate specifically on the nonresonant multiphoton ionization of the rare gases argon, krypton, and xenon at a fixed laser frequency. In a separate experiment,^{1,2} utilizing the second harmonic of the same laser, strong resonant enhancement of the multiphoton ionization rate was observed at intensities exceeding 10^{13} W/cm².

The experiment consists of the measurement of the actual numbers of ions produced in the various charge states (e.g., Ar⁺, Ar⁺², etc.) as functions of laser intensity. The emphasis on the measurement of the absolute yield of ions produced in each charge state is dictated by the desire to perform a direct quantitative comparison of the experimental results with theory. The wavelength used was 586 nm. This frequency exhibited no discernible multiphoton resonant behavior in any of the target species over the intensity range investigated.

Details of the experimental configuration have been described elsewhere.³ Briefly, the laser system consists of a well diagnosed amplified, synchronously pumped dye laser. The system provides 1-2-psec pulses which are continuously tunable from 570 to 620 nm. Pulse energies are typically 3 mJ with an approximately 10% amplified spontaneous-emission component spread over the range 580 to 583 nm. The pulses are transform limited ($\Delta\nu\Delta\tau = 0.29 \pm 0.04$) with approximately 80% of the

pulse energy contained in the lowest-order spatial mode. The laser is focused by a 6.3-cm focal-length lens which yields a very nearly Gaussian distribution at the focus with a $1/e^2$ diameter of 20 μ m. A fraction of the laser pulse is passed through a thin angle-tuned KDP crystal to produce a small amount of second-harmonic radiation. Both the second harmonic and laser energy are measured on every shot. Combined, these measurements yield the peak power on each shot (see Ref. 3). Since the spatial distribution at the focus does not change from shot to shot, a measurement of the actual intensity on target on every shot is obtained.

The final lens is located inside the target chamber which has a residual background pressure of $\leq 1 \times 10^{-7}$ Torr. The target species is introduced into the chamber by a high-precision leak valve to a pressure of typically 2×10^{-6} Torr and fills the chamber uniformly. The ions are analyzed with a time-of-flight spectrometer which

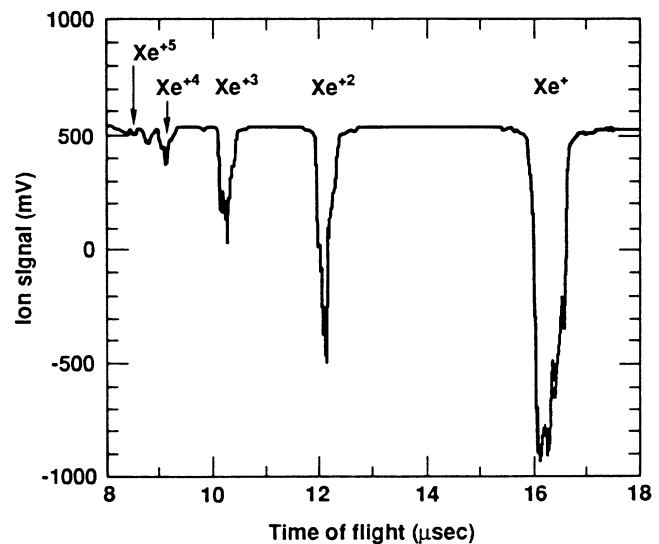


FIG. 1. Typical time-of-flight spectrum of xenon at a peak intensity of 2×10^{14} W/cm² ($P_{Xe} = 2.67 \times 10^{-6}$ Torr).

was designed to resolve completely the isotope structure of natural xenon. A uniform electric field of 5000 V/cm is applied across the interaction region to extract any ion formed at the laser focus. The ions are detected by direct impact on a 2.5-cm-diam microchannel plate. The ion spectrum is recorded on every shot by a fast transient digitizer and a series of gated integrators.

An experimental run consists of our acquiring between 2000 and 3000 laser shots over an intensity range of 10^{13} to 4×10^{14} W/cm². A typical time-of-flight spectrum is shown in Fig. 1. The actual number of ions being detected in a given charge state is obtained by normalization of the integrated signal to the single-ion signal of each charge state. The number of ions produced may then be calculated with use of the overall detection efficiency. This was measured to be $6 \pm 2\%$.

The results for Ar and Xe are shown in Fig. 2. As ex-

plained above, great care was taken to obtain a good calibration of both the laser intensity and absolute ion yield to allow direct quantitative comparison with theory. The combined systematic error in pulse energy, pulse width, and spatial distribution measurements is estimated to be less than 50%. The general shape of the curves is similar to that observed in previous experiments⁴ and can be explained as follows: When the ion yield is relatively low, the parent atom or ion population is not depleted anywhere in the focal volume and the ion yield is dependent only on some power of the peak intensity, I_0 . In perturbation theory, this power is simply N_0 , the minimum number of photons required to ionize the parent. When the ionization probability approaches unity, the parent species becomes depleted throughout the focal volume. Further contribution to the ion yield comes from the expanding focal volume which grows

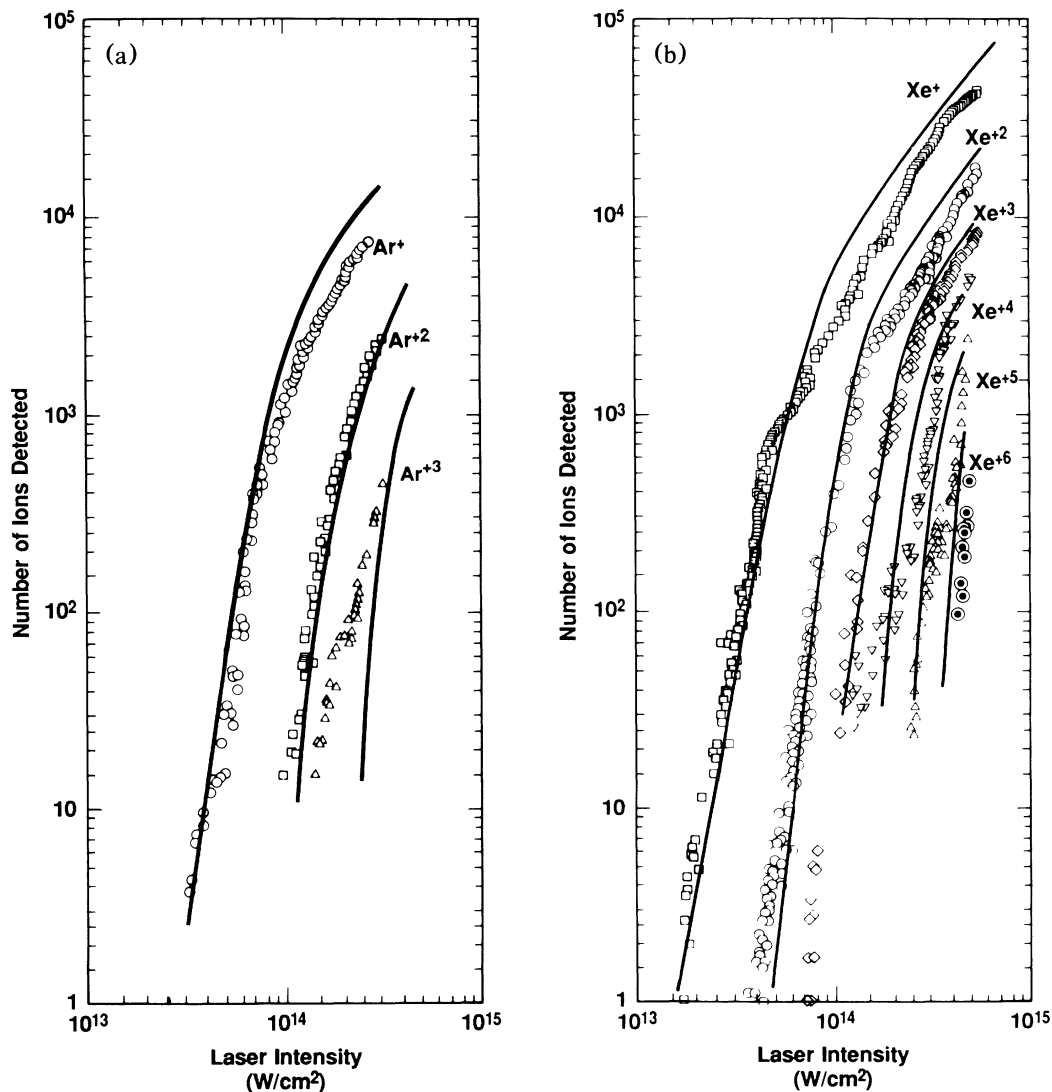


FIG. 2. Detected absolute ion yield of (a) Ar and (b) Xe as a function of laser intensity. The solid curves are the results of direct calculations as described in the text.

asymptotically as $I_0^{3/2}$.

Similar measurements were made for krypton. The threshold intensity, defined as the intensity at which the ionization probability is 10^{-4} , is plotted as a function of ionization potential in Fig. 3. The smooth increase in threshold intensity for the production of the higher charge states is a general result, independent of the atomic or ionic system investigated. This suggests that the nonresonant ionization rate is a fairly weak function of the details of the atomic structure. In fact, it appears that the ionization rate is determined primarily by a gross feature of the atom, its binding energy.

The threshold intensity for xenon is more than an order of magnitude larger than that observed in an earlier experiment performed at 532 nm.⁴ However, recent measurements of the threshold intensity in Xe at 620 nm were found to be within 20% of our measurements at 586 nm.⁵ The large difference between the earlier measurements of L'Huillier *et al.* at 532 nm and those reported here is not understood at present.

Our expression for the ionization rate can be derived in a manner similar to Keldysh,⁶ Reiss,⁷ and Faisal⁸ (see Perry⁹), or from a more general approach.¹⁰ The expression can be written in a form similar to the well-known Fermi "golden rule,"

$$W = (2\pi/\hbar) |\langle \psi_f | H_{\text{int}} | \psi_i \rangle|^2 \rho(E_f) \delta(E_f - E_i - N\hbar\omega), \quad (1)$$

where the wave functions, ψ_i and ψ_f , denote the initial and final states of the system, and $\rho(E_f)$ is the density of final states. The energies, E_i and E_f , are the quasienergies of the initial and final states, respectively. The interaction Hamiltonian in radiation gauge and the dipole approximation is

$$H_{\text{int}} = \frac{-e}{mc} \mathbf{p} \cdot \mathbf{A} + \frac{e^2}{2mc^2} (|\mathbf{A}|^2 - \langle |\mathbf{A}|^2 \rangle), \quad (2)$$

$$\frac{dW}{d\Omega} = \left(\frac{1}{2\pi} \right)^2 \left(\frac{2m^2\omega^5}{\hbar^3} \right)^{1/2} \sum_{n=N_0}^{\infty} \frac{n^2(n-n_b-n_{\text{osc}})}{(n-n_{\text{osc}})^{1/2}} |\phi_i(\mathbf{p})|^2 J_n^2(n_f, -\frac{1}{2}n_{\text{osc}}), \quad (3)$$

where $J_n(n_f, -\frac{1}{2}n_{\text{osc}})$ are generalized Bessel functions,⁷ $\phi_i(\mathbf{p})$ is the wave function of the initial state in momentum space, n_b is the ratio of the ionization potential P to the energy of the photon, $P/\hbar\omega$, $n_{\text{osc}} = e^2|\mathcal{A}|^2/4mc^2\hbar\omega$, and $n_f = [8n_{\text{osc}}(n-n_{\text{osc}})]^{1/2}\mu$, $\mu = \cos\theta$, where θ is the angle between the propagation direction of the outgoing electron and the polarization vector of the field. The magnitude of the local momentum of the outgoing electron is given by $|\mathbf{p}| = [p_0^2 + 2mP(0)]^{1/2}$, where $p_0 = [2m(n\hbar\omega - P)]^{1/2}$, $P(0)$ is the field-free ionization potential, and IP is the ionization potential of the atom in the field, $P = P(0) + n_{\text{osc}}\hbar\omega$. The minimum number of photons required to ionize the atom, N_0 , is simply the first integer which exceeds $n_b + n_{\text{osc}}$.¹²

This expression is similar in form to that of Reiss, and, in fact, reduces to his expression in the limit that the Coulomb field of the residual ion is zero. Taking the initial state to be hydrogenic with a binding energy equal to the ionization potential and integrating Eq. (3) over all solid angles yields

$$W = 32\omega n_b^{5/2} \sum_{n=N_0}^{\infty} \frac{n^2(n-n_b-n_{\text{osc}})}{(n-n_{\text{osc}})^{1/2}(n+n_b-n_{\text{osc}})^4} \int_0^1 J_n^2(n_f, -\frac{1}{2}n_{\text{osc}}) d\mu. \quad (4)$$

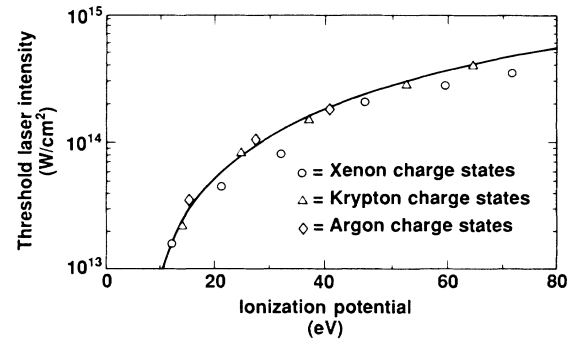


FIG. 3. Threshold laser intensity, defined as the intensity at which the ionization probability is 10^{-4} , as a function of the ionization potential of a given charge state.

where the vector potential is given by $\mathbf{A} = \mathcal{A}(t)\cos\omega t$, and ω is the frequency of the applied monochromatic field. The time average of the vector potential, $\langle |\mathbf{A}|^2 \rangle$, is subtracted out of the time-dependent interaction Hamiltonian so as not to be counted twice. The multiphoton character of the ionization is hidden in the wave functions, ψ_i and ψ_f , which are "dressed" by several photons.

Equation (1) is evaluated under the assumption that the applied field affects only a single electron, leaving the remaining electrons in their initial state. The ac Stark shifts of the ground states of the atom and ion are neglected. The Coulomb field of the residual ion is accounted for by our taking the final state as the WKB wave function of an electron in a constant potential subject to an intense electromagnetic field (a modified Volkov state¹¹). The magnitude of the potential is equal to the ionization potential of the initial state. The density of final states and the energy of the outgoing electron are obtained from the local momentum of the electron in this constant potential.⁹ Under these approximations, the ionization rate into a solid angle $d\Omega$ for a linearly polarized field can be written

The individual terms in this expression correspond to the total ionization rate from the various "above-threshold ionization" channels.¹³⁻¹⁵

A computer code was written which evaluates Eq. (4) and obtains the energy distribution of the photoelectrons for a given laser intensity. The program then uses the ionization rates at a given laser intensity to integrate a series of rate equations with the empirically determined $\text{sech}^2(2t/\tau_p)$ temporal and Gaussian spatial distributions of the laser pulse. The total number of ions detected is obtained by integration of the solution to the rate equations over volume and multiplication of the result by overall detection efficiency. The results of these calculations for charge states up to Ar^{3+} , Kr^{5+} , and Xe^{6+} are shown as the solid curves in Figs. 2 and 3. This extended Keldysh-Reiss-Faisal theory is in good agreement with our experimental results for charge states up to Ar^{2+} , Kr^{3+} , and Xe^{4+} . Charge states higher than these exhibit a generally lower threshold intensity than that predicted by the theory. In addition, it should be noted that the constant potential employed here will be a poor approximation to the residual Coulomb potential experienced by the outgoing electron for fields of high intensity and frequencies beyond the near infrared as the excursions of the electron from the nucleus under these conditions can be substantial.

In conclusion, we have measured the absolute yields of multiply charged ions of the rare gases, Ar, Kr, and Xe, produced by nonresonant multiphoton ionization at $\lambda = 586$ nm as functions of laser intensity in the range $10^{13} \leq I \leq 4 \times 10^{14}$ W/cm² using a picosecond dye laser system. When the multiphoton ionization is nonresonant, the "threshold intensity," defined as the intensity at which the ionization probability is 10^{-4} , is a smooth, monotonic function of the ionization potential. This suggests that the ionization rate is a fairly weak function of the details of the atomic or ionic structure. Calculations for the production of multiply charged ions involving a model of sequential ionization with rates obtained from a theory similar to that of Keldysh, but which accounts for

the Coulomb field of the residual ion, are within the experimental errors. To our knowledge, these calculations represent the best agreement to date between theory and experiment on the nonresonant multiphoton ionization rates of the noble gases. Our model has recently been applied to the experimental results of others^{5,15} and again found to be in good agreement with no adjustable parameters.

We would like to thank H. Szoke for writing the computer code. We would also like to thank A. L'Huillier, P. Bucksbaum, and P. Corkum for many helpful discussions.

¹O. L. Landen, M. D. Perry, and E. M. Campbell, *Phys. Rev. Lett.* **59**, 2558 (1987).

²M. D. Perry, O. L. Landen, and E. M. Campbell, to be published.

³M. D. Perry, O. L. Landen, A. Szoke, and E. M. Campbell, *Phys. Rev. A* **37**, 747 (1988).

⁴A. L'Huillier, L. A. Lompre, G. Mainfray, and C. Manus, *J. Phys. B* **16**, 1363 (1983), and *Phys. Rev. A* **27**, 2503 (1983).

⁵P. Corkum, to be published.

⁶L. V. Keldysh, *Zh. Eksp. Teor. Fiz.* **47**, 1945 (1964) [*Sov. Phys. JETP* **20**, 1307 (1965)].

⁷H. R. Reiss, *Phys. Rev. A* **22**, 1786 (1980).

⁸F. H. M. Faisal, *J. Phys. B* **6**, L89 (1973).

⁹M. D. Perry, Ph.D. thesis, University of California, Berkeley, 1987 (unpublished).

¹⁰A. Szoke, University of California Report No. UCRL-95294, 1987 (to be published).

¹¹D. M. Volkov, *Z. Phys.* **94**, 250 (1935).

¹²A different correction to Keldysh's work has been suggested by P. H. Bucksbaum, private communication.

¹³P. Agostini, F. Fabre, G. Mainfray, and G. Petite, *Phys. Rev. Lett.* **42**, 1127 (1979).

¹⁴P. Kruit, J. Kimman, H. G. Muller, and M. J. van der Wiel, *Phys. Rev. A* **28**, 248 (1983).

¹⁵T. J. McIlrath, P. H. Bucksbaum, R. R. Freeman, and M. Bashkansky, *Phys. Rev. A* **35**, 4611 (1987).